Biochimica et Biophysica Acta 1848 (2015) 1699–1705

Contents lists available at ScienceDirect

Biochimica et Biophysica Acta

journal homepage: www.elsevier.com/locate/bbamem

Cholesterol-induced changes in hippocampal membranes utilizing a phase-sensitive fluorescence probe

Roopali Saxena [1], Sandeep Shrivastava [1], Amitabha Chattopadhyay *

CSIR—Centre for Cellular and Molecular Biology, Uppal Road, Hyderabad 500 007, India

ARTICLE INFO

Article history:
Received 23 February 2015
Received in revised form 20 April 2015
Accepted 5 May 2015
Available online 8 May 2015

Keywords:
Hippocampal membrane
Membrane cholesterol
MβCD
NR12S
REES

ABSTRACT

The function of membrane receptors in the nervous system depends on physicochemical characteristics of neuronal membranes such as membrane order and phase. In this work, we have monitored the changes in hippocampal membrane order and related parameters by cholesterol and protein content utilizing a Nile Red-based phase-sensitive fluorescent membrane probe NR12S. Since alteration of membrane cholesterol is often associated with membrane phase change, the phase-sensitive nature of NR12S fluorescence becomes useful in these experiments. Our results show that fluorescence spectroscopic parameters such as emission maximum, anisotropy, and lifetime of NR12S display characteristic dependence on membrane cholesterol content. Interestingly, cholesterol-dependent red edge excitation shift is displayed by NR12S under these conditions. Hippocampal membranes exhibited reduction in liquid-ordered phase upon cholesterol depletion. These results provide insight into changes in hippocampal membrane order in the overall context of cholesterol and protein modulation.

1. Introduction

Organization of neuronal membranes is crucial in the context of the function of receptors embedded in them, particularly in view of the unique membrane lipid composition in the nervous system [1,2]. In this context, cholesterol is a physiologically relevant lipid since brain cholesterol has been implicated in a number of neurological disorders [3–5]. It is known that the function of neuronal receptors is modulated by cholesterol [6–9], which affects neurotransmission and gives rise to mood and anxiety disorders [10]. A number of neurological disorders share a common etiology of defective cholesterol metabolism in the brain [11]. A hallmark of membrane cholesterol is its nonrandom localization in domains in biological and model membranes [12–14]. Cholesterol is unique in its ability to form liquid-ordered-like phases in higher eukaryotic plasma membranes [15]. In this overall context, exploring neuronal membrane organization in relation to membrane cholesterol modulation assumes relevance.

We recently reported the location, dynamics, and environment-sensitive properties of a novel Nile Red-based phase-sensitive membrane probe (NR12S) [16]. We further showed, utilizing model membranes of varying phases, that important fluorescence parameters such as emission maximum, red edge excitation shift (REES), anisotropy and lifetime of NR12S exhibit sensitivity to the membrane phase. In our laboratory, we have established hippocampal membranes as a primary source for studying the interaction of neuronal receptors such as the serotonin$_{1A}$ receptor with membrane lipids [17,18]. An important finding from these studies is that cholesterol-induced membrane organization is necessary for the function of neuronal receptors [7–9,18]. Since alteration of membrane cholesterol is often associated with membrane phase change, in this work, we utilized the phase-sensitive membrane probe NR12S to explore the changes in organization and dynamics of hippocampal membranes under conditions of varying cholesterol content.

2. Materials and methods

2.1. Materials

Cholesterol, 1,2-dimyristoyl-*sn*-glycero-3-phosphocholine (DMPC), EDTA, EGTA, $MgCl_2$, $MnCl_2$, Na_2HPO_4, iodoacetamide, PMSF, sucrose, sodium azide, Tris and methyl-β-cyclodextrin (MβCD) were purchased from Sigma Chemical Co. (St. Louis, MO). Bicinchoninic acid (BCA) assay reagent for protein estimation was from Pierce (Rockford, IL). Amplex Red cholesterol assay kit was from Molecular Probes/Invitrogen (Eugene, OR). NR12S was synthesized as described previously [19]. The concentration of a stock solution of NR12S prepared in DMSO was estimated using its molar extinction coefficient (ε) of 45,000 M^{-1} cm^{-1} at 550 nm in ethanol. All other chemicals used were of the highest purity available. Solvents used were of spectroscopic grade. Water was purified through a Millipore (Bedford, MA) Milli-Q system and used throughout. Fresh bovine brains were obtained from a local slaughterhouse within

Abbreviations: BCA, bicinchoninic acid; DMPC, 1,2-dimyristoyl-*sn*-glycero-3-phosphocholine; MβCD, methyl-β-cyclodextrin; Nile Red, 9-diethylamino-5H-benzo[α]phenoxazine-5-one; PMSF, phenylmethylsulfonyl fluoride; REES, red edge excitation shift; Tris, *tris*-(hydroxymethyl)aminomethane

* Corresponding author. Tel.: +91 40 2719 2578; fax: +91 40 2716 0311.
E-mail address: amit@ccmb.res.in (A. Chattopadhyay).
[1] These authors contributed equally to this work.

http://dx.doi.org/10.1016/j.bbamem.2015.05.001
0005-2736/

10 min of death and the hippocampal region was carefully dissected out. The hippocampi were immediately flash frozen in liquid nitrogen and stored at −70 °C until further use.

2.2. Methods

2.2.1. Preparation of native hippocampal membranes

Native hippocampal membranes were prepared as described previously [18], flash frozen in liquid nitrogen and stored at −70 °C. Protein concentration was assayed using BCA reagent with bovine serum albumin as standard [20].

2.2.2. Cholesterol depletion of native hippocampal membranes

Native hippocampal membranes were depleted of cholesterol using MβCD as described previously [18,21]. Cholesterol content was estimated using the Amplex Red assay kit [22].

2.2.3. Lipid extraction from native and cholesterol-depleted membranes

Lipid extraction was carried out from native and cholesterol-depleted hippocampal membranes as described previously [23] using a modified Bligh and Dyer method [24]. The lipid extract was finally dissolved in a chloroform–methanol mixture (1:1, v/v).

2.2.4. Estimation of phospholipids

Concentration of lipid phosphate was determined subsequent to total digestion by perchloric acid using Na_2HPO_4 as standard [25]. DMPC was used as an internal standard to assess lipid digestion. Samples without perchloric acid digestion produced negligible readings.

2.2.5. Sample preparation

Membranes (native and cholesterol-depleted) containing 100 nmol of total phospholipid were suspended in 2 ml of 10 mM Tris buffer (pH 7.4). NR12S was added from a stock solution in DMSO such that the final probe concentration was 1 mol% with respect to the total phospholipid content. The resultant probe concentration was 0.5 μM in all cases and the DMSO content was always low (<0.1%, v/v). This ensures optimal fluorescence intensity with negligible membrane perturbation. NR12S was added to membranes while being vortexed for 1 min at room temperature (~23 °C). Samples were kept in the dark for 1 h before measurements. Background samples were prepared the same way except that NR12S was omitted.

Lipid extracts containing 100 nmol of total phospholipid in chloroform–methanol (1:1, v/v) were mixed well with 1 nmol of NR12S in DMSO. Samples were mixed well and dried under a stream of nitrogen while being warmed gently (~45 °C). After further drying under a high vacuum for at least 6 h, 2 ml of 10 mM Tris, pH 7.4 buffer was added, and lipid samples were hydrated (swelled) at ~70 °C while being intermittently vortexed for 3 min to disperse the lipid and form homogeneous multilamellar vesicles (MLVs). The MLVs were kept at ~70 °C for an additional hour to ensure proper swelling as the vesicles were formed. Such high temperatures were necessary for hydrating the samples due to the presence of lipids with high melting temperature in neuronal tissues [26]. Samples were kept in the dark at room temperature (~23 °C) overnight prior to fluorescence measurements.

2.2.6. Steady state fluorescence measurements

Steady state fluorescence measurements were performed with a Hitachi F-7000 spectrofluorometer (Tokyo, Japan) using 1 cm path length quartz cuvettes. Excitation and emission slits with a bandpass of 5 nm were used for all measurements. Background intensities of samples in which NR12S was omitted were subtracted from each sample spectrum to cancel out any contribution due to the solvent Raman peak and other scattering artifacts. The spectral shifts obtained with different sets of samples were identical in most cases. In other cases, the values were within ±1 nm of those reported.

Fluorescence anisotropy measurements were performed at room temperature (~23 °C) using a Hitachi Glan–Thompson polarization accessory. Anisotropy values were calculated from the equation [27]:

$$r = \frac{I_{VV} - GI_{VH}}{I_{VV} + 2GI_{VH}} \quad (1)$$

where I_{VV} and I_{VH} are the fluorescence intensities (after appropriate background subtraction) measured with the excitation polarizer oriented vertically and the emission polarizer vertically and horizontally oriented, respectively. G is the grating factor and is the ratio of the efficiencies of the detection system for vertically and horizontally polarized light, and is equal to I_{HV}/I_{HH}.

2.2.7. Time-resolved fluorescence measurements

Fluorescence lifetimes were calculated from time-resolved fluorescence intensity decays using IBH 5000F NanoLED equipment (Horiba Jobin Yvon, Edison, NJ) with DataStation software in the time-correlated single photon counting (TCSPC) mode. A pulsed light-emitting diode (LED) (NanoLED-01) was used as an excitation source. This LED generates optical pulse at 490 nm with pulse duration 1.2 ns and is run at 1 MHz repetition rate. The LED profile (instrument response function) was measured at the excitation wavelength using Ludox (colloidal silica) as the scatterer. To optimize the signal-to-noise ratio, 10,000 photon counts were collected in the peak channel. All experiments were performed using emission slits with bandpass of 8 nm. The sample and the scatterer were alternated after every 5% acquisition to ensure compensation for shape and timing drifts occurring during the period of data collection. This arrangement also prevents any prolonged exposure of the sample to the excitation beam, thereby avoiding any possible photodamage of the fluorophore. Data were stored and analyzed using DAS 6.2 software (Horiba Jobin Yvon, Edison, NJ). Fluorescence intensity decay curves so obtained were deconvoluted with the instrument response function and analyzed as a sum of exponential terms

$$F(t) = \Sigma_i \alpha_i \exp(-t/\tau_i) \quad (2)$$

where F(t) is the fluorescence intensity at time t and α_i is a pre-exponential factor representing the fractional contribution to the time-resolved decay of the component with a lifetime of τ_i such that $\Sigma_i \alpha_i = 1$. The program also includes statistical and plotting subroutine packages [28]. The goodness of the fit of a given set of observed data and the chosen function was evaluated by the χ^2 ratio, the weighted residuals [29], and the autocorrelation function of the weighted residuals [30]. A fit was considered acceptable when plots of the weighted residuals and the autocorrelation function showed random deviation about zero with a minimum χ^2 value not more than 1.5. Intensity-averaged mean lifetimes $\langle\tau\rangle$ for biexponential decays of fluorescence were calculated from the decay times and pre-exponential factors using the equation [27]:

$$\langle\tau\rangle = \frac{\alpha_1\tau_1^2 + \alpha_2\tau_2^2}{\alpha_1\tau_1 + \alpha_2\tau_2}. \quad (3)$$

3. Results and discussion

Cholesterol content of hippocampal membranes can be conveniently modulated using MβCD by selective extraction of cholesterol from hippocampal membranes by including it in the central nonpolar cavity [18,31]. Fig. 1 shows that cholesterol content in hippocampal membranes gets progressively reduced upon treatment with increasing concentrations of MβCD. Upon treatment with 10 mM MβCD, cholesterol content was reduced to ~83% of the control. The extent of cholesterol depletion was highest when 40 mM MβCD was used, with cholesterol content being reduced to ~15% of the control. Fig. 1 shows

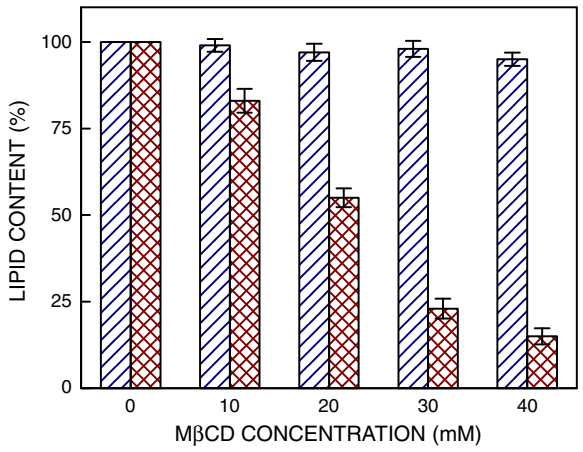

Fig. 1. Effect of MβCD on the lipid content of hippocampal membranes. The figure shows phospholipid (hatched bar) and cholesterol (crisscrossed bar) contents in hippocampal membranes treated with increasing concentrations of MβCD. Values are expressed as percentages of phospholipid and cholesterol contents in native hippocampal membranes without MβCD treatment. Data represent means ± S.E. of at least four independent measurements. See Materials and methods for other details.

that the membrane phospholipid level remains invariant under these conditions.

NR12S (see inset in Fig. 2 for chemical structure) is a fluorescent membrane probe based on Nile Red. Nile Red is a popular probe whose fluorescence properties are sensitive to the polarity of its immediate environment since there is large change in its dipole moment upon excitation [32,33]. The advantage of NR12S over Nile Red is that it has unique orientation and location in the membrane due to the additional fatty acyl chain that helps in anchoring of the molecule in the membrane [19]. We recently showed, using the parallax approach [34], that the fluorophore in NR12S is localized at the membrane interface, characterized by an average depth of penetration of ~18 Å from the center of the bilayer [16]. In addition, NR12S has the advantage of being localized exclusively in the outer leaflet of the membrane [35,36]. More importantly, NR12S fluorescence displays sensitivity to the membrane phase [16,19].

Membrane phase is an important determinant of membrane physical properties [37]. While the lipid fatty acyl chains are ordered and

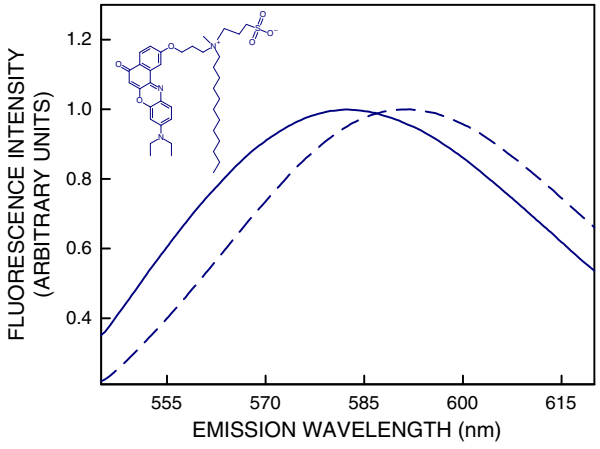

Fig. 2. Representative fluorescence emission spectra of NR12S in native (———) and cholesterol-depleted (- - - - -) hippocampal membranes. The concentration of MβCD used was 40 mM. The spectra are intensity-normalized at the respective emission maxima. Measurements were carried out at room temperature (~23 °C). The excitation wavelength used was 510 nm. The ratio of NR12S to total lipid was 1:100 (mol/mol). The chemical structure of NR12S is also shown. See Materials and methods for other details.

extended in all transconformation in the gel (ordered) phase, they are fluid and disordered in the liquid-disordered phase. The liquid-ordered phase, on the other hand, represents an interesting phase, and is characterized by extended (ordered) acyl chains (like the gel phase), but display high lateral mobility similar to the liquid-disordered phase [15,40]. The liquid-ordered phase exists above a threshold level of cholesterol for binary lipid mixtures [15]. Hippocampal membranes are neuronal in origin, and are rich in protein and cholesterol [38]. A number of approaches that include fluorescence polarization of membrane probes [18], wavelength dependence of Laurdan generalized polarization (GP) [39], and order parameters from electron spin resonance (ESR) spectra of spin-labeled phospholipids [23] showed that the native hippocampal membrane is in the liquid-ordered phase. The apparent liquid-ordered nature of hippocampal membranes could be due to high cholesterol content (~31 mol%) in these membranes [38]. The fluorescence emission spectra of NR12S in native and cholesterol-depleted (using 40 mM MβCD) hippocampal membranes are shown in Fig. 2. The fluorescence emission maximum was observed at ~581 and 591 nm in native and cholesterol-depleted hippocampal membranes, respectively. The red shift in the emission spectrum of NR12S could be due to reduction in liquid-ordered phase induced by cholesterol depletion [16,19].

REES is defined as the shift in the wavelength of maximum fluorescence emission toward higher wavelengths, caused by a shift in the excitation wavelength toward the red edge of the absorption band. This effect is significant for fluorophores with a relatively large change in dipole moment upon excitation in restricted environment (for recent reviews on REES and its applications, see [41,42]). An attractive aspect of REES is that it allows to monitor the mobility parameters of the environment itself (represented by the relaxing solvent molecules) using the fluorophore merely as a reporter group. REES has proved to be a useful tool to monitor probe environment in membranes and membrane-mimetic environments [43–48].

The shifts in fluorescence emission maxima of NR12S with increasing excitation wavelength in hippocampal membranes with varying cholesterol content and in liposomes of lipid extract from these membranes are shown in Fig. 3 (panels A and B) and corresponding REES in each case is shown in Fig. 4. Upon depletion of cholesterol from hippocampal membranes using varying concentrations (10–40 mM) of MβCD, the fluorescence emission maximum of NR12S exhibited progressive red shift toward longer wavelengths. The emission maximum corresponding to hippocampal membranes treated with 10, 20, 30 and 40 mM MβCD was 584, 589, 590 and 591 nm, respectively (excitation wavelength was 510 nm in all cases). The highest red shift (10 nm) was obtained when maximum cholesterol was depleted using 40 mM MβCD (see Fig. 1), although there was a leveling off at higher concentrations of MβCD. The red shift in emission maximum is possibly due to an increase in apparent polarity experienced by the fluorophore, possibly because of increase in water penetration in the membrane induced by cholesterol depletion, as previously reported using polarity-sensitive vibronic peak ratio of pyrene [49]. The magnitudes of REES displayed by hippocampal membranes with varying cholesterol content are shown in Figs. 3A and 4. Fig. 4 shows that REES decreases upon increasing cholesterol depletion, *i.e.*, from 15 nm (native hippocampal membranes) to 9 nm (hippocampal membranes treated with 40 mM MβCD). Hippocampal membranes with intermediate cholesterol concentrations showed REES of 13 (treated with 10 mM MβCD), 9 (20 mM MβCD) and 8 (30 mM MβCD) nm. Observation of REES in these membranes suggests that the fluorophore in NR12S experiences motionally restricted environment.

Corresponding data for liposomes of lipid extract from these membranes are shown in Figs. 3B and 4. The emission maximum of NR12S in control liposomes from lipid extracts (without cholesterol depletion) was observed at 581 nm, similar to native hippocampal membranes. Since the emission maximum of NR12S remains unaltered (at 581 nm) in hippocampal membranes and in liposomes of lipid extract

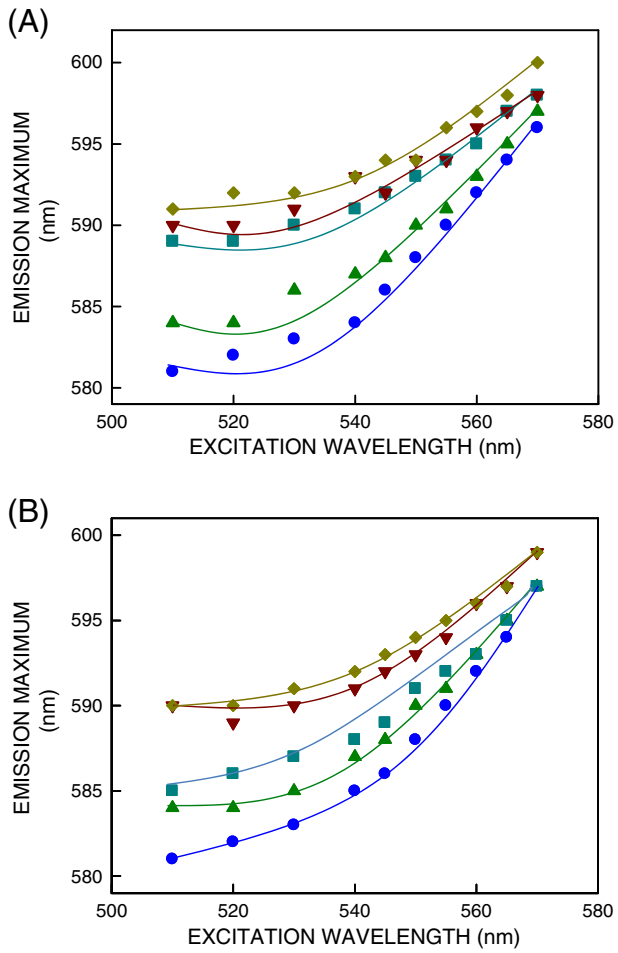

Fig. 3. Effect of changing excitation wavelength on the wavelength of maximum emission of NR12S in (A) native hippocampal membranes, and (B) liposomes of lipid extract from native membranes. Data corresponding to control (●), and membranes treated with 10 (▲), 20 (■), 30 (▼), 40 (♦) mM MβCD are shown. The lines joining the data points are provided merely as viewing guides. All other conditions are as in Fig. 2. See Materials and methods for other details.

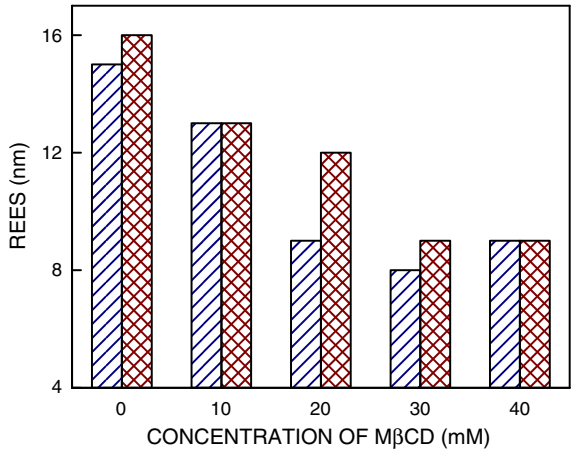

Fig. 4. Effect of cholesterol depletion on the magnitude of REES of NR12S in native hippocampal membranes, and in liposomes of lipid extract from native membranes. REES of NR12S, corresponding to total shift in emission maximum when the excitation wavelength was changed from 510 to 570 nm, in native membranes (hatched bar) and in liposomes of lipid extract (crisscrossed bar) from native membranes are shown with increasing cholesterol depletion using 10–40 mM MβCD. All other conditions are as in Fig. 2. See Materials and methods for other details.

from native membranes, it appears that the emission maximum is not sensitive to the presence of proteins (see below). As seen with hippocampal membranes, the emission maximum was progressively red shifted from 581 nm (control membranes) to 590 nm in case of liposomes of lipid extracts from hippocampal membranes treated with 40 mM MβCD. For liposomes of lipid extracts from hippocampal membranes treated with 10, 20, and 30 mM MβCD, the emission maximum was observed at 584, 585, and 590 nm, respectively. The magnitude of REES for these membranes is shown in Fig. 4. REES changes from 16 nm (no cholesterol depletion) to 9 nm, corresponding to maximal cholesterol depletion. Comparable extents of REES observed in hippocampal membranes and in liposomes from lipid extracts from these membranes (both with varying cholesterol content) suggest that proteins do not significantly contribute to motional restriction of the environment in these membranes in fluorescence time scale. Interestingly, we have previously reported that proteins in hippocampal membranes do not significantly contribute to membrane heterogeneity, as monitored by lifetime distribution of the fluorescent probe Nile Red [50]. Taken together, these results provide support for lipid vesicles as good biological membrane models.

Fluorescence anisotropy is known to depend on the excitation wavelength in motionally restricted environment [51]. The rotational rate of the fluorophore is reduced in the relaxed state due to strong dipolar interactions with the surrounding solvent molecules. Upon excitation at the red edge, this subclass of fluorophores gets selectively excited. Due to strong interaction with the polar solvent molecules with this subpopulation of fluorophores in the excited state, these 'solvent relaxed' fluorophores rotate more slowly, thereby increasing anisotropy. The excitation anisotropy spectra of NR12S in hippocampal membranes with varying amounts of cholesterol are shown in Fig. 5A. As shown in the figure, the anisotropy of NR12S in these membranes shows considerable increase upon increasing the excitation wavelength from 510 to 570 nm in all cases. Similar trend was exhibited in liposomes of lipid extracts from these membranes (see Fig. 5B). Fig. 6A shows the change in anisotropy of NR12S in hippocampal membranes with varying cholesterol content with increasing emission wavelength. Considerable reduction in anisotropy with increasing emission wavelength is observed in all cases. Such reduction in anisotropy across the emission spectrum is associated with fluorophores in motionally restricted media [51]. The change in anisotropy of NR12S with increasing emission wavelength in liposomes of lipid extracts from these membranes is comparable (see Fig. 6B).

Fluorescence anisotropy is commonly used to monitor the rotational diffusion rate of membrane embedded probes, which is sensitive to membrane packing [27,52]. This is due to the fact that fluorescence anisotropy depends on the extent to which the probe is able to reorient after excitation, and probe reorientation is dependent on membrane packing. Fig. 7 shows that the anisotropy of NR12S in native (control) hippocampal membranes is ~0.20. The anisotropy is progressively reduced with increasing cholesterol depletion and reaches a value of ~0.17 in hippocampal membranes treated with 40 mM MβCD. The reduction in anisotropy with cholesterol depletion could be due to altered membrane packing giving rise to reduced membrane order. The anisotropy of NR12S in liposomes of lipid extracts from these membranes displayed a similar trend.

Fluorescence lifetime serves as a sensitive indicator of the local environment in which a given fluorophore is localized [53]. A typical decay profile of NR12S in liposomes of lipid extract from native membranes with its biexponential fitting and the statistical parameters used to check the goodness of the fit is shown in Fig. S1 (see Supplementary material). The lifetimes of NR12S in hippocampal membranes of varying cholesterol content and in liposomes of lipid extract from these membranes are shown in Table 1. All fluorescence decays obtained could be fitted well to a biexponential function. We chose to use the intensity-averaged mean fluorescence lifetime as an important parameter since it is independent of the method of analysis and the number

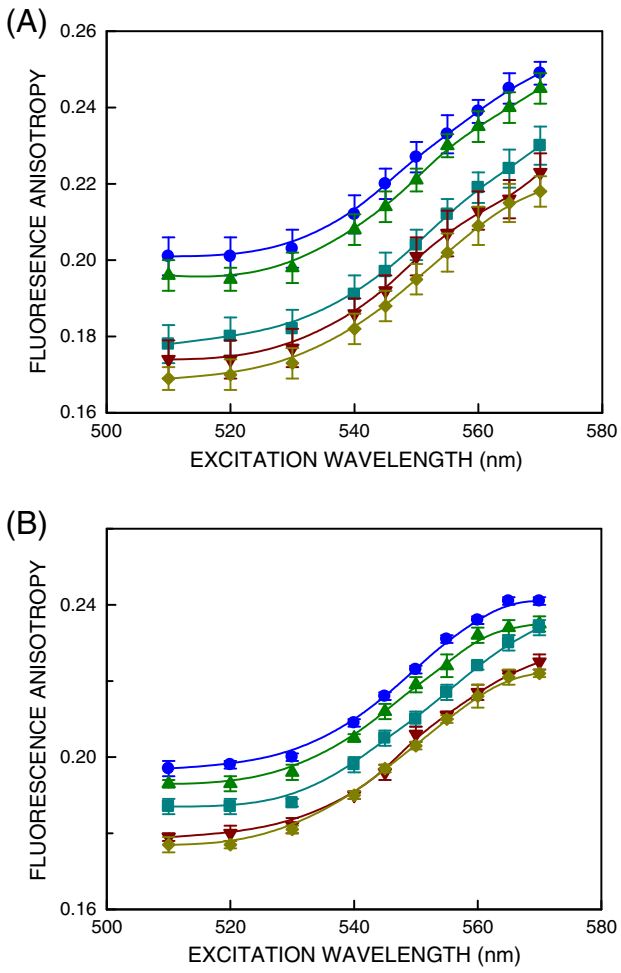

Fig. 5. Fluorescence anisotropy with increasing excitation wavelength for NR12S in (A) native hippocampal membranes, and (B) liposomes of lipid extract from native membranes. Data corresponding to control (●), and membranes treated with 10 (▲), 20 (■), 30 (▼), 40 (♦) mM MβCD are shown. The lines joining the data points are provided merely as viewing guides. The emission wavelength was 585 nm in all cases. All other conditions are as in Fig. 2. Data points shown are the means ± S.E. of at least three independent measurements. See Materials and methods for other details.

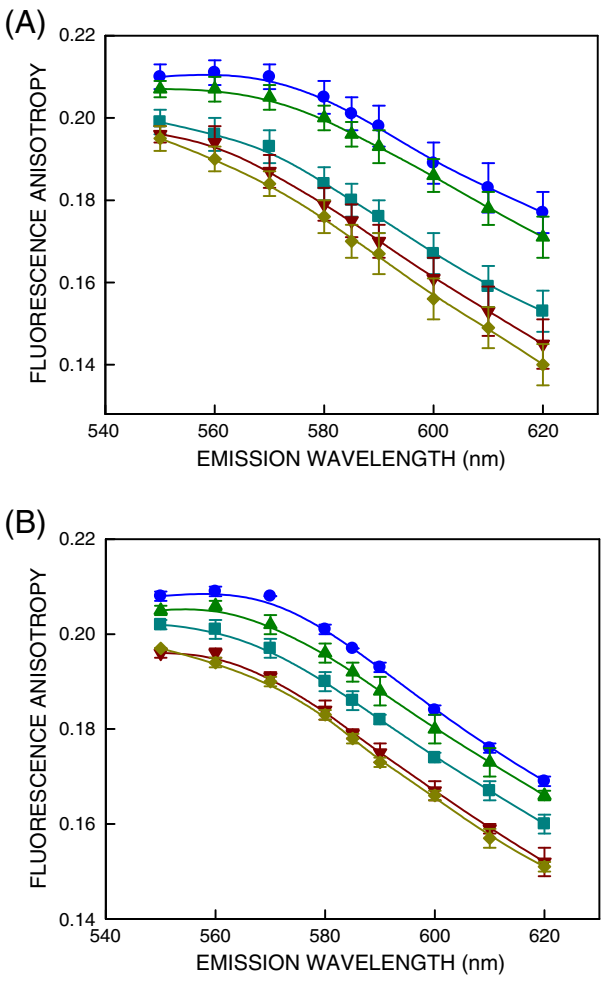

Fig. 6. Fluorescence anisotropy with increasing emission wavelength for NR12S in (A) native hippocampal membranes, and (B) liposomes of lipid extract from native membranes. Data corresponding to control (●), and membranes treated with 10 (▲), 20 (■), 30 (▼), 40 (♦) mM MβCD are shown. The lines joining the data points are provided merely as viewing guides. The excitation wavelength was 520 nm in all cases. All other conditions are as in Fig. 2. Data points shown are the means ± S.E. of at least three independent measurements. See Materials and methods for other details.

of exponentials used to fit the time-resolved fluorescence decay. The mean fluorescence lifetimes of NR12S in hippocampal membranes of varying cholesterol content and in lipid extracts were calculated from data shown in Table 1 using Eq. (3) and are shown in Fig. 8A. The mean fluorescence lifetime of NR12S was found to be ~4.4 and 4.3 ns in native hippocampal membranes and in liposomes of lipid extract from hippocampal membranes, respectively. The mean fluorescence lifetime of NR12S displayed progressive reduction upon increasing extent of cholesterol depletion in both hippocampal membranes and in lipid extracts from these membranes (see Fig. 8A). This reduction in mean fluorescence lifetime could be due to an increase in polarity experienced by the probe upon cholesterol depletion due to an increase in water penetration in the membrane. We have previously shown that fluorescence lifetime of NR12S is sensitive to polarity of the surrounding environment and lifetime of NR12S decreases with increasing polarity [16].

To rule out the fact that anisotropy values of NR12S (Fig. 7) were affected by lifetime-induced artifacts, the apparent (average) rotational correlation times were calculated using Perrin's equation [27]:

$$\tau_c = \frac{\langle \tau \rangle r}{r_o - r} \quad (4)$$

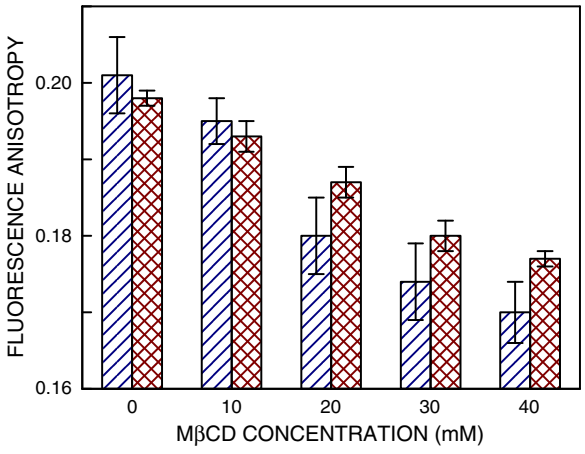

Fig. 7. Effect of cholesterol depletion on fluorescence anisotropy of NR12S in native hippocampal membranes and in liposomes of lipid extract from native membranes. Fluorescence anisotropy of NR12S in native membranes (hatched bar) and in liposomes of lipid extract (crisscrossed bar) from native membranes are shown with increasing cholesterol depletion (using 10–40 mM MβCD). All other conditions are as in Fig. 2. See Materials and methods for other details.

Table 1
Fluorescence lifetimes of NR12S in hippocampal membranes and lipid extract with varying cholesterol content.[a]

Concentration of MβCD (mM)	α_1	τ_1 (ns)	α_2	τ_2 (ns)
Native membranes				
0	0.14	1.50	0.86	4.52
10	0.12	1.28	0.88	4.44
20	0.19	1.43	0.81	4.28
30	0.22	1.25	0.78	4.02
40	0.24	1.27	0.76	3.85
Lipid extract				
0	0.14	1.33	0.86	4.38
10	0.17	1.30	0.83	4.30
20	0.21	1.37	0.79	4.16
30	0.21	1.30	0.79	3.98
40	0.23	1.21	0.77	3.92

[a] The excitation wavelength was 490 nm and emission was monitored at 585 nm. The number of photons collected at the peak channel was 10,000. All other conditions are as in Fig. 8. See Materials and methods for other details.

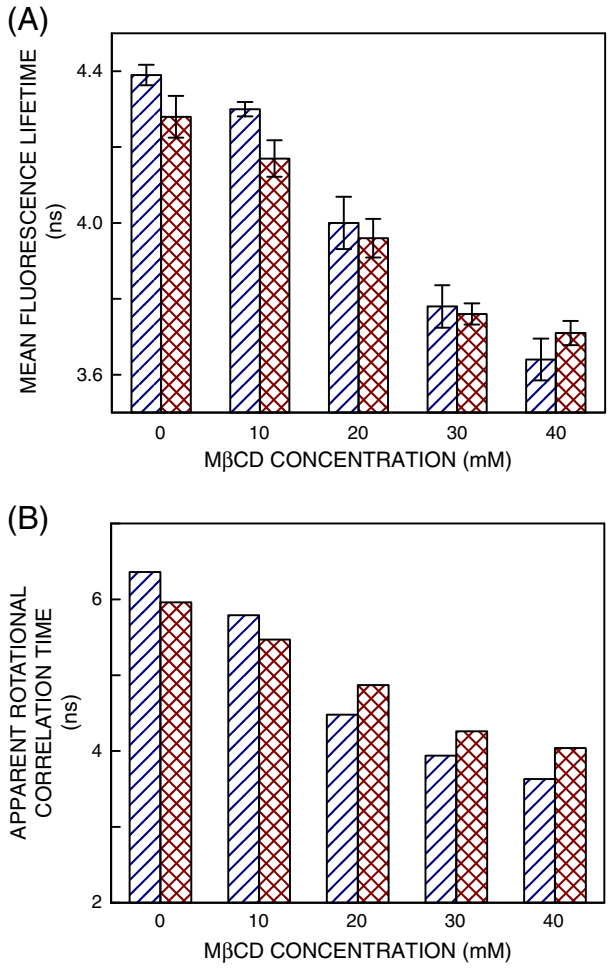

Fig. 8. (A) Effect of cholesterol depletion on mean fluorescence lifetime of NR12S in native hippocampal membranes (hatched bar) and in liposomes of lipid extract from native membranes (crisscrossed bar). Mean fluorescence lifetimes were calculated using Eq. (3). The excitation wavelength used was 490 nm and emission was monitored at 585 nm. Data shown are means ± S.E. of at least three independent measurements. All other conditions are as in Fig. 2. See Materials and methods for other details. (B) Apparent rotational correlation times of NR12S in native hippocampal membranes (hatched bar) and in liposomes of lipid extract from native membranes (crisscrossed bar) with increasing cholesterol depletion. Apparent rotational correlation times were calculated from fluorescence anisotropy values of NR12S from Fig. 7 and mean fluorescence lifetimes from panel (A) using Eq. (4). See text for other details.

where r_o is the limiting (fundamental) anisotropy of the fluorophore in the absence of any other depolarizing processes such as rotational diffusion, r is the steady state anisotropy (taken from Fig. 7), and $\langle\tau\rangle$ is the mean fluorescence lifetime from Fig. 8A. The values of the apparent rotational correlation times, calculated using Eq. (4) with r_o value of 0.34 [54], are shown in Fig. 8B. The figure shows that the apparent rotational correlation time was maximum in native hippocampal membranes and showed progressive reduction with increasing cholesterol depletion (also in liposomes of lipid extracts from these membranes). The observation that apparent rotational correlation times displayed a trend similar to that observed for fluorescence anisotropy (see Fig. 7), ensured that the reported changes in anisotropy values are not influenced by lifetime.

Taken together, we report here the modulation of the organization and dynamics of hippocampal membranes by membrane cholesterol and proteins utilizing the phase-sensitive fluorescent probe NR12S. Our results show that fluorescence parameters such as emission maximum, red edge excitation shift (REES), anisotropy and lifetime are dependent on membrane cholesterol content and phase. Hippocampal membranes showed reduction in liquid-ordered phase upon cholesterol depletion. Interestingly, NR12S exhibits REES that is dependent on membrane cholesterol content. Since the fluorescence moiety of NR12S is located at the interfacial region of membrane [16], our results provide information about the organization and dynamics of this functionally important region of the membrane in the overall context of cholesterol and protein depletion. An interesting feature emerging from these results is that proteins do not contribute significantly to the organization and dynamics of hippocampal membranes in the time scale probed.

The interaction between membrane lipids (such as cholesterol and sphingolipids) and neurotransmitter receptors in neuronal membranes is important for understanding brain function [3,6]. Knowledge of neuronal membrane physicochemical parameters such as membrane order and phase would be useful in analyzing functional data on membrane receptors obtained by modulation of membrane lipid composition [18,55]. These results could have implications in neuronal diseases such as the Smith–Lemli–Opitz syndrome [11,56,57], which is characterized by defective cholesterol biosynthesis.

Supplementary data to this article can be found online at http://dx.doi.org/10.1016/j.bbamem.2015.05.001.

Conflict of interest

The authors declare that there is no conflict of interest.

Acknowledgments

This work was supported by the Council of Scientific and Industrial Research (CSIR, India) Network project MIND (BSC0115) to A.C. We sincerely thank Dr. Andrey Klymchenko for the kind gift of NR12S. R.S. thanks CSIR for the award of a Senior Research Fellowship. A.C. is an Adjunct Professor of Jawaharlal Nehru University (New Delhi, India) and Indian Institute of Science Education and Research (Mohali, India), Indian Institute of Technology (Kanpur) and Honorary Professor at the Jawaharlal Nehru Centre for Advanced Scientific Research (Bangalore, India). A.C. gratefully acknowledges J.C. Bose Fellowship (Department of Science and Technology, Government of India). We thank the members of the Chattopadhyay laboratory for critically reading the manuscript.

References

[1] P.S. Sastry, Lipids of nervous tissue: composition and metabolism, Prog. Lipid Res. 24 (1985) 69–176.
[2] M.R. Wenk, The emerging field of lipidomics, Nat. Rev. Drug Discov. 4 (2005) 594–610.

[3] A. Chattopadhyay, Y.D. Paila, Lipid–protein interactions, regulation and dysfunction of brain cholesterol, Biochem. Biophys. Res. Commun. 354 (2007) 627–633.
[4] M. Martin, C.G. Dotti, M.D. Ledesma, Brain cholesterol in normal and pathological aging, Biochim. Biophys. Acta 1801 (2010) 934–944.
[5] M.G. Martín, F. Pfrieger, C.G. Dotti, Cholesterol in brain disease: sometimes determinant and frequently implicated, EMBO Rep. 15 (2014) 1036–1052.
[6] J.A. Allen, R.A. Halverson-Tamboli, M.M. Rasenick, Lipid raft microdomains and neurotransmitter signalling, Nat. Rev. Neurosci. 8 (2007) 128–140.
[7] T.J. Pucadyil, A. Chattopadhyay, Role of cholesterol in the function and organization of G-protein coupled receptors, Prog. Lipid Res. 45 (2006) 295–333.
[8] Y.D. Paila, A. Chattopadhyay, Membrane cholesterol in the function and organization of G-protein coupled receptors, Subcell. Biochem. 51 (2010) 439–466.
[9] M. Jafurulla, A. Chattopadhyay, Membrane lipids in the function of serotonin and adrenergic receptors, Curr. Med. Chem. 20 (2013) 47–55.
[10] G.I. Papakostas, D. Öngür, D.V. Iosifescu, D. Mischoulon, M. Fava, Cholesterol in mood and anxiety disorders: review of the literature and new hypotheses, Eur. Neuropsychopharmacol. 14 (2004) 135–142.
[11] F.D. Porter, G.E. Herman, Malformation syndromes caused by disorders of cholesterol synthesis, J. Lipid Res. 52 (2011) 6–34.
[12] X. Xu, E. London, The effect of sterol structure on membrane lipid domains reveals how cholesterol can induce lipid domain formation, Biochemistry 39 (2000) 843–849.
[13] D. Lingwood, K. Simons, Lipid rafts as a membrane-organizing principle, Science 327 (2010) 46–50.
[14] A. Chaudhuri, A. Chattopadhyay, Transbilayer organization of membrane cholesterol at low concentrations: implications in health and disease, Biochim. Biophys. Acta 1808 (2011) 19–25.
[15] O.G. Mouritsen, The liquid-ordered state comes of age, Biochim. Biophys. Acta 1798 (2010) 1286–1288.
[16] R. Saxena, S. Shrivastava, S. Haldar, A.S. Klymchenko, A. Chattopadhyay, Location, dynamics and solvent relaxation of a nile red-based phase-sensitive fluorescent membrane probe, Chem. Phys. Lipids 183 (2014) 1–8.
[17] K.G. Harikumar, A. Chattopadhyay, Metal ion and guanine nucleotide modulations of agonist interaction in G-protein-coupled serotonin$_{1A}$ receptors from bovine hippocampus, Cell. Mol. Neurobiol. 18 (1998) 535–553.
[18] T.J. Pucadyil, A. Chattopadhyay, Cholesterol modulates ligand binding and G-protein coupling to serotonin$_{1A}$ receptors from bovine hippocampus, Biochim. Biophys. Acta 1663 (2004) 188–200.
[19] O.A. Kucherak, S. Oncul, Z. Darwich, D.A. Yushchenko, Y. Arntz, P. Didier, Y. Mély, A.S. Klymchenko, Switchable nile red-based probe for cholesterol and lipid order at the outer leaflet of biomembranes, J. Am. Chem. Soc. 132 (2010) 4907–4916.
[20] P.K. Smith, R.I. Krohn, G.T. Hermanson, A.K. Mallia, F.H. Gartner, M.D. Provenzano, E.K. Fujimoto, N.M. Goeke, B.J. Olson, D.C. Klenk, Measurement of protein using bicinchoninic acid, Anal. Biochem. 150 (1985) 76–85.
[21] P. Singh, Y.D. Paila, A. Chattopadhyay, Differential effects of cholesterol and 7-dehydrocholesterol on the ligand binding activity of the hippocampal serotonin$_{1A}$ receptor: implications in SLOS, Biochem. Biophys. Res. Commun. 358 (2007) 495–499.
[22] D.M. Amundson, M. Zhou, Fluorometric method for the enzymatic determination of cholesterol, J. Biochem. Biophys. Methods 38 (1999) 43–52.
[23] P. Singh, P.K. Tarafdar, M.J. Swamy, A. Chattopadhyay, Organization and dynamics of hippocampal membranes in a depth-dependent manner: an electron spin resonance study, J. Phys. Chem. B 116 (2012) 2999–3006.
[24] E.G. Bligh, W.J. Dyer, A rapid method of total lipid extraction and purification, Can. J. Biochem. Physiol. 37 (1959) 911–917.
[25] C.W.F. McClare, An accurate and convenient organic phosphorus assay, Anal. Biochem. 39 (1971) 527–530.
[26] R. Koynova, M. Caffrey, Phases and phase transitions of the sphingolipids, Biochim. Biophys. Acta 1255 (1995) 213–236.
[27] J.R. Lakowicz, Principles of Fluorescence Spectroscopy, 3rd ed. Springer, New York, 2006.
[28] D.V. O'Connor, D. Phillips, Time-correlated Single Photon Counting, Academic Press, London, 1984. 180–189.
[29] R.A. Lampert, L.A. Chewter, D. Phillips, D.V. O'Connor, A.J. Roberts, S.R. Meech, Standards for nanosecond fluorescence decay time measurements, Anal. Chem. 55 (1983) 68–73.
[30] A. Grinvald, I.Z. Steinberg, On the analysis of fluorescence decay kinetics by the method of least-squares, Anal. Biochem. 59 (1974) 583–598.
[31] P. Singh, S. Haldar, A. Chattopadhyay, Differential effect of sterols on dipole potential in hippocampal membranes: implications for receptor function, Biochim. Biophys. Acta 1828 (2013) 917–923.
[32] P. Greenspan, S.D. Fowler, Spectrofluorometric studies of the lipid probe, nile red, J. Lipid Res. 26 (1985) 781–789.
[33] C.M. Golini, B.W. Williams, J.B. Foresman, Further solvatochromic, thermochromic, and theoretical studies on Nile Red, J. Fluoresc. 8 (1998) 395–404.
[34] A. Chattopadhyay, E. London, Parallax method for direct measurement of membrane penetration depth utilizing fluorescence quenching by spin-labeled phospholipids, Biochemistry 26 (1987) 39–45.
[35] S. Chiantia, A.S. Klymchenko, E. London, A novel leaflet-selective fluorescence labeling technique reveals differences between inner and outer leaflets at high bilayer curvature, Biochim. Biophys. Acta 1818 (2012) 1284–1290.
[36] Z. Darwich, A.S. Klymchenko, O.A. Kucherak, L. Richert, Y. Mély, Detection of apoptosis through the lipid order of the outer plasma membrane leaflet, Biochim. Biophys. Acta 1818 (2012) 3048–3054.
[37] G. van Meer, D.R. Voelker, G.W. Feigenson, Membrane lipids: where they are and how they behave, Nat. Rev. Mol. Cell Biol. 9 (2008) 112–124.
[38] T.J. Pucadyil, A. Chattopadhyay, Exploring detergent insolubility in bovine hippocampal membranes: a critical assessment of the requirement for cholesterol, Biochim. Biophys. Acta 1661 (2004) 9–17.
[39] S. Mukherjee, A. Chattopadhyay, Monitoring the organization and dynamics of bovine hippocampal membranes utilizing Laurdan generalized polarization, Biochim. Biophys. Acta 1714 (2005) 43–55.
[40] D.A. Brown, E. London, Structure and origin of ordered lipid domains in biological membranes, J. Membr. Biol. 164 (1998) 103–114.
[41] S. Haldar, A. Chaudhuri, A. Chattopadhyay, Organization and dynamics of membrane probes and proteins utilizing the red edge excitation shift, J. Phys. Chem. B 115 (2011) 5693–5706.
[42] A. Chattopadhyay, S. Haldar, Dynamic insight into protein structure utilizing red edge excitation shift, Acc. Chem. Res. 47 (2014) 12–19.
[43] A. Chattopadhyay, S. Mukherjee, Depth-dependent solvent relaxation in membranes: wavelength-selective fluorescence as a membrane dipstick, Langmuir 15 (1999) 2142–2148.
[44] S.S. Rawat, A. Chattopadhyay, Structural transition in the micellar assembly: a fluorescence study, J. Fluoresc. 9 (1999) 233–244.
[45] H. Raghuraman, S.K. Pradhan, A. Chattopadhyay, Effect of urea on the organization and dynamics of Triton X-100 micelles: a fluorescence approach, J. Phys. Chem. B 108 (2004) 2489–2496.
[46] D.A. Kelkar, A. Chattopadhyay, Depth-dependent solvent relaxation in reverse micelles: a fluorescence approach, J. Phys. Chem. B 108 (2004) 12151–12158.
[47] S. Mukherjee, A. Chattopadhyay, Influence of ester and ether linkage in phospholipids on the environment and dynamics of the membrane interface: a wavelength-selective fluorescence approach, Langmuir 21 (2005) 287–293.
[48] S. Shrivastava, S. Haldar, G. Gimpl, A. Chattopadhyay, Orientation and dynamics of a novel fluorescent cholesterol analogue in membranes of varying phase, J. Phys. Chem. B 113 (2009) 4475–4481.
[49] R. Saxena, S. Shrivastava, A. Chattopadhyay, Exploring the organization and dynamics of hippocampal membranes utilizing pyrene fluorescence, J. Phys. Chem. B 112 (2008) 12134–12138.
[50] S. Mukherjee, M. Kombrabail, G. Krishnamoorthy, A. Chattopadhyay, Dynamics and heterogeneity of bovine hippocampal membranes: role of cholesterol and proteins, Biochim. Biophys. Acta 1768 (2007) 2130–2144.
[51] S. Mukherjee, A. Chattopadhyay, Wavelength-selective fluorescence as a novel tool to study organization and dynamics in complex biological systems, J. Fluoresc. 5 (1995) 237–246.
[52] D.M. Jameson, J.A. Ross, Fluorescence polarization/anisotropy in diagnostics and imaging, Chem. Rev. 110 (2010) 2685–2708.
[53] F.G. Prendergast, Time-resolved fluorescence techniques: methods and applications in biology, Curr. Opin. Struct. Biol. 1 (1991) 1054–1059.
[54] M.L. Ferrer, F. del Monte, Enhanced emission of nile red fluorescent nanoparticles embedded in hybrid sol–gel glasses, J. Phys. Chem. B 109 (2005) 80–86.
[55] Y.D. Paila, M.R.V.S. Murty, M. Vairamani, A. Chattopadhyay, Signaling by the human serotonin$_{1A}$ receptor is impaired in cellular model of Smith–Lemli–Opitz syndrome, Biochim. Biophys. Acta 1778 (2008) 1508–1516.
[56] F.D. Porter, Smith–Lemli–Opitz syndrome: pathogenesis, diagnosis and management, Eur. J. Hum. Genet. 16 (2008) 535–541.
[57] A.E. DeBarber, Y. Eroglu, L.S. Merkens, A.S. Pappu, R.D. Steiner, Smith–Lemli–Opitz syndrome, Expert Rev. Mol. Med. 13 (2011) e24.